# SYNTHESIS OF INVERSE FILTERS WITH PROJECTED DYNAMICAL SYSTEMS

**K. Kuhnen**

Laboratory for Process Automation (LPA)
Saarland University, Building 13
D-66123 Saarbrücken, Germany
fax: +49-681-302-2678 and e-mail: k.kuhnen@lpa.uni-saarland.de

**Keywords:** Inverse filters, projected dynamical systems, identification, convex constraints, hysteresis compensation

## Abstract

The present paper describes a procedure for synthesising an inverse filter for a complex hysteretic nonlinearity as it occurs in active materials such as piezoelectric ceramics, magnetostrictive materials and shape memory alloys using the so-called modified Prandtl-Ishlinskii approach. In this synthesis procedure the parameters of an appropriate linear error model have to be optimised in a convex polyhedron to ensure the existence of the corresponding inverse filter. As in future work concerned with iterative and adaptive compensation strategies the determination of the parameters should be performed on-line, the solution of the underlying convex quadratic programming problem is formulated as the global exponentially stable equilibrium point of a properly projected dynamical system.

## 1 Introduction

The ongoing miniaturisation of mechatronic systems requires, in addition to the sensor principles which can be miniaturised, also actuators with a high energy density to be able to achieve sufficiently high forces in small sites. This requirement is largely fulfilled by actuators made of magnetostrictive and piezoelectric materials, shape memory alloys, by electromagnetic actuators and so on. But one of the greatest problems in control is the complex hysteretic characteristic of sensors and actuators, which causes a non-linear and multi-valued mapping between the output variable and the input variable of the transducer. Thereby the non-linear and multi-valued relation between the corresponding input and output variables has a very different characteristic depending on the type of the actuator [1]. One possibility to handle this problem is to compensate the hysteretic actuator characteristic in open loop control by using an inverse feed-forward filter. To obtain a sufficiently precise compensation of the hysteretic nonlinearity the hysteretic characteristic of the actuator has to be identified and inverted before operation.

In the past few years a general modeling and compensator design method was developed for such complex hysteretic nonlinearities based on the so-called modified Prandtl-Ishlinskii approach [2,3]. A fundamental problem in the identification of complex hysteretic nonlinearities not only with the modified Prandtl-Ishlinskii approach but also with the well-known Preisach approach is given by the fact that compensators exist only in a certain set of the model parameter space [6]. Because the underlying error model of the modified Prandtl-Ishlinskii approach depends linearly on the error model parameters, and the restrictions can be formulated through inequality constraints, the admissible solution set for the parameters is a convex polyhedron, and the corresponding identification problem to be solved is a convex quadratic program. For solving these well conditioned problems before putting the control system into operation the optimisation theory provides multiple powerful algorithms. But these algorithms are not suitable for optimisation during operation of the control system, because they require too much computing power. A possibility to avoid these difficulties is to formulate the solution of the bounded quadratic optimisation problem as a stable equilibrium point in a proper system of differential equations. This dynamical system can then be solved through numerical integration very efficiently from time step to time step during the operation of the control system. In the unbounded case, for instance, the right-hand side of the demanded differential equation is given by the negative gradient of the quadratic target function.

The main subject of this paper is the extension of this negative gradient approach to the bounded case for which the theory of projected dynamical systems [4] offers a starting point. The right-hand side of the differential equation follows in this case from a projection of the negative gradient which ensures that the trajectory of the system under no circumstances leaves the admissible solution set. In contrast to parameter projection methods normally used in the field of adaptive systems, the applied projection transformation considers also the non-differentiability points at the boundaries of the convex solution set. As in the case of a convex polyhedron these non-differentiability points often result from the intersection of smooth convex sets.

## 2 Solution of quadratic programs with dynamical systems

Optimisation problems

$$\min_{\boldsymbol{w}\in K}\{V(\boldsymbol{w})\} \tag{1}$$

with

$$V(\boldsymbol{w}) = \frac{1}{2}\boldsymbol{w}^T \cdot \boldsymbol{H} \cdot \boldsymbol{w} + \boldsymbol{g}^T \cdot \boldsymbol{w} + f \qquad (2)$$

and

$$K = \left\{ \boldsymbol{w} \in \Re^d \;\middle|\; \boldsymbol{U} \cdot \boldsymbol{w} - \boldsymbol{u} \geq \boldsymbol{o} \right\}, \qquad (3)$$

$\boldsymbol{H} \in \Re^{d \times d}$, $\boldsymbol{g} \in \Re^d$, $f \in \Re$, $\boldsymbol{U} \in \Re^{m \times d}$ and $\boldsymbol{u} \in \Re^m$ are called quadratic programs (QP) and are an integral part of various identification and synthesis procedures for open-loop and closed-loop control systems, whose underlying error model is linearly dependent on the error model parameters $\boldsymbol{w}$ and whose parameters are bounded by a convex polyhedron $K$. If $\boldsymbol{H}$ is positive-definite the quadratic program is strictly convex and the solution set of the minimisation problem (1) - (3) consists of only one solution point [5].

### 2.1 Optimality conditions for bounded quadratic optimisation problems

The necessary and sufficient condition for a minimum value $\boldsymbol{w}_* \in K$ of a strictly convex quadratic function (2) results from the consideration that in a minimum $\boldsymbol{w}_*$ the function $V$ must not decrease for all feasible variations $\boldsymbol{z} - \boldsymbol{w}_*$, $\boldsymbol{z} \in K$. This means that in the minimum $\boldsymbol{w}_*$ the variation $\Delta V$ of the function $V$ must obey the variational inequality

$$\Delta V(\boldsymbol{w}_*) = \nabla V(\boldsymbol{w}_*)^T \cdot (\boldsymbol{z} - \boldsymbol{w}_*) \geq 0 \;\;,\;\; \forall \boldsymbol{z} \in K \,. \qquad (4)$$

If the minimum of a strictly convex quadratic function lies outside the feasible set $K$, then $\nabla V(\boldsymbol{w}) \neq \boldsymbol{o}$ holds for all $\boldsymbol{w} \in K$ and the fulfillment of the variational inequality depends only on the direction of $\nabla V(\boldsymbol{w})$ at a boundary point $\boldsymbol{w} \in \partial K$. In this case the variational inequality is fulfilled if

$$-\nabla V(\boldsymbol{w}) \in C(\boldsymbol{w}) \qquad (5)$$

holds. The set

$$C(\boldsymbol{w}) = \left\{ \boldsymbol{v} \in \Re^d \;\middle|\; \boldsymbol{v}^T \cdot (\boldsymbol{z} - \boldsymbol{w}) \leq 0 \,,\, \forall \boldsymbol{z} \in K \right\} \qquad (6)$$

is called the outward normal cone of $K$ at the point $\boldsymbol{w}$. If the minimum of the quadratic function lies inside or on the boundary of the feasibility set $K$, then there exists a unique $\boldsymbol{w}_* \in K$ with $\nabla V(\boldsymbol{w}_*) = \boldsymbol{o}$ and the variational inequality (4) is fulfilled independently of the direction of $\boldsymbol{z} - \boldsymbol{w}_*$.

### 2.2 Projection mapping

In the optimisation literature many different algorithms exist for the solution of the quadratic program (1) - (3) which cannot be implemented during system operation because of their high demand on computation resources [5]. The differential equation with gradient vector field

$$\dot{\boldsymbol{w}}(t) = -\nabla V(\boldsymbol{w}(t)) \;\;,\;\; \boldsymbol{w}(0) = \boldsymbol{w}_0 \in \Re^d \qquad (7)$$

used for the solution of unbounded quadratic optimisation problems during system operation has to be extended in such a way that (a) the unbounded case is included as a special case, (b) the solution trajectory remains in the feasible region, (c) the nondiferentiability points of the boundary are considered and (d) the equilibrium point coincides with the solution of the variational inequality (4).

A key role for fulfilling these requirements is played by the projection of the vector $\boldsymbol{v} \in \Re^d$ at the point $\boldsymbol{w} \in K$ to $K$ defined by

$$\boldsymbol{Q}_K(\boldsymbol{w}, \boldsymbol{v}) = \lim_{\delta \to 0} \frac{\boldsymbol{Q}(\boldsymbol{w} + \delta \boldsymbol{v}) - \boldsymbol{w}}{\delta} \qquad (8)$$

with

$$\boldsymbol{Q}(\boldsymbol{w}) = \min_{\boldsymbol{Q} \in K} \left\| \boldsymbol{w} - \boldsymbol{Q} \right\|_2 \qquad (9)$$

[4]. Fig. 1 explains the geometrical interpretation of the projection mapping $\boldsymbol{Q}_K$ for a nondifferentiability point $\boldsymbol{w} \in \partial K$ of the boundary $\partial K$. For $\boldsymbol{v} \in C(\boldsymbol{w})$ follows $\boldsymbol{Q}_K = \boldsymbol{o}$, see fig. 1b.

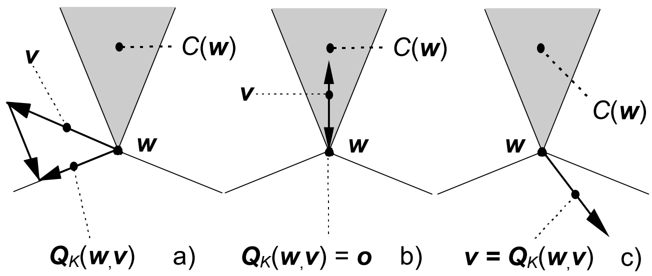


**Figure 1:** Geometrical interpretation of the projection mapping $\boldsymbol{Q}_K$

In the case $\boldsymbol{v} \notin C(\boldsymbol{w})$ and $\boldsymbol{w} + \boldsymbol{v} \notin K$ the direction of $\boldsymbol{Q}_K$ coincides with the direction of the feasible variation $\boldsymbol{z} - \boldsymbol{w}$, $\boldsymbol{z} \in K$ which has the smallest distance to $\boldsymbol{v}$, see fig. 1a. If the vector $\boldsymbol{v}$ lies within the feasible region then $\boldsymbol{Q}_K$ and $\boldsymbol{v}$ coincides. This is shown in fig. 1c.

### 2.3 Differential equation with projected gradient vector field

With the projection mapping (8) a type of differential equation

$$\dot{\boldsymbol{w}}(t) = \boldsymbol{Q}_K(\boldsymbol{w}(t), -\nabla V(\boldsymbol{w}(t))) \;\;,\;\; \boldsymbol{w}(0) = \boldsymbol{w}_0 \in K \qquad (10)$$

can be defined which belongs to the class of so-called projected dynamical systems [4]. At the equilibrium points $\boldsymbol{w}_\infty \in K$ of (10) the left-hand side of the differential equation vanishes. Thus the equilibrium points fulfill the equation

$$\boldsymbol{o} = \boldsymbol{Q}_K(\boldsymbol{w}_\infty, -\nabla V(\boldsymbol{w}_\infty)) \,. \qquad (11)$$

The relationship between the equilibrium points $\boldsymbol{w}_\infty \in K$ of the differential equation (10) and the solution points $\boldsymbol{w}_* \in K$ of the variational inequality (4) is formulated by theorem 2.4 of [4]. According to this theorem the equilibrium points $\boldsymbol{w}_\infty \in K$ of the differential equation (10) coincide with the solution points $\boldsymbol{w}_* \in K$ of the variational inequality (4), if the feasible region $K$ is a convex polyhedron (3). A statement about the stability properties of the equilibrium points $\boldsymbol{w}_\infty \in K$ of the differential equation (10) can be formulated with theorem 3.7 of [4]. For this purpose the following stability notion is used: An equilibrium point $\boldsymbol{w}_\infty \in K$ of the differential equation (10) is called *globally exponentially stable*, if there exist constants $D > 0$ and $\lambda > 0$, such that for all $\boldsymbol{w}_0 \in K$

$$\|\boldsymbol{w}(t) - \boldsymbol{w}_\infty\| \le D\|\boldsymbol{w}_0 - \boldsymbol{w}_\infty\| e^{-\lambda t}\,. \tag{12}$$

The stability properties of the equilibrium points $\boldsymbol{w}_\infty \in K$ of (10) are strongly influenced by the properties of the gradient $\nabla V(\boldsymbol{w})$. If the Hessian matrix $\nabla\nabla V(\boldsymbol{w})$ is *strongly positive-definite* in the whole region $K$, it follows

$$\boldsymbol{q}^T \cdot \nabla\nabla V(\boldsymbol{w}) \cdot \boldsymbol{q} \ge \eta \|\boldsymbol{q}\|^2 \quad \forall\, \boldsymbol{q} \in \Re^d \;\wedge\; \forall\, \boldsymbol{w} \in K \tag{13}$$

with $\eta > 0$. In this case $\nabla V(\boldsymbol{w})$ is called *strongly globally monotone* in $K$ and the equilibrium point $\boldsymbol{w}_\infty \in K$ of (10) is globally exponentially stable. Due to (2) the stability properties of the equilibrium points $\boldsymbol{w}_\infty \in K$ of (10) are given by

$$\nabla\nabla V(\boldsymbol{w}) = \boldsymbol{H} \tag{14}$$

and thus are determined by the definiteness properties of the matrix $\boldsymbol{H}$. For a positive-definite matrix $\boldsymbol{H}$ follows

$$\boldsymbol{q}^T \cdot \boldsymbol{H} \cdot \boldsymbol{q} \ge \min\{\lambda_i(\boldsymbol{H})\}\|\boldsymbol{q}\|^2 \quad \forall\, \boldsymbol{q} \in \Re^d\,, \tag{15}$$

and the differential equation (10) has exactly one globally exponentially stable equilibrium point $\boldsymbol{w}_\infty \in K$. According to this $\min\{\lambda_i(\boldsymbol{H})\}$ is the smallest positive real eigenvalue of the matrix $\boldsymbol{H}$.

## 3 Filter synthesis with the modified Prandtl-Ishlinskii approach

The modified Prandtl-Ishlinskii hysteresis operator has been developed recently for the modeling and compensation of asymmetrically complex hysteretic nonlinearities [2,3]. It is defined as the concatenation of a Prandtl-Ishlinskii hysteresis operator $H$ and a Prandtl-Ishlinskii superposition operator $S$ and in vector notation is given by

$$\begin{aligned}\Gamma[x](t) &= S[H[x]](t)\\ &= \boldsymbol{w}_S^{\,T} \cdot \boldsymbol{S}_{r_S}[\boldsymbol{w}_H^{\,T} \cdot \boldsymbol{H}_{r_H}[x, \boldsymbol{z}_{H0}]](t).\end{aligned} \tag{16}$$

The operator $H$ consists of a weighted linear superposition of $n$+1 elementary play operators $H_{rH}$, which are included in (16) in the $n$+1-dimensional vector $\boldsymbol{H}_{rH}$. The rate-independent characteristic of the play is characterised by the threshold-dependent $x$-$y$-trajectory, see fig. 2a. The weights $w_{Hi}$, the thresholds $r_{Hi}$ and the initial values $z_{H0i}$, $i = 0 \,..\, n$ of the play operators are considered in the vector notation (16) by the vector of weights $\boldsymbol{w}_H^{\,T} = (w_{H0}\; w_{H1} \,..\, w_{Hn})$, the vector of thresholds $\boldsymbol{r}_H^{\,T} = (r_{H0}\; r_{H1} \,..\, r_{Hn})$ with $r_{H0} = 0$ and the vector of the initial values $\boldsymbol{z}_{H0}^{\,T} = (z_{H00}\; z_{H01} \,..\, z_{H0n})$. The outputs of the elementary operators $z_{Hi} = H_{rH}[x, z_{H0i}]$, $i = 0 \,..\, n$ represent the inner system state or the memory of the discrete-threshold Prandtl-Ishlinskii hysteresis operator.

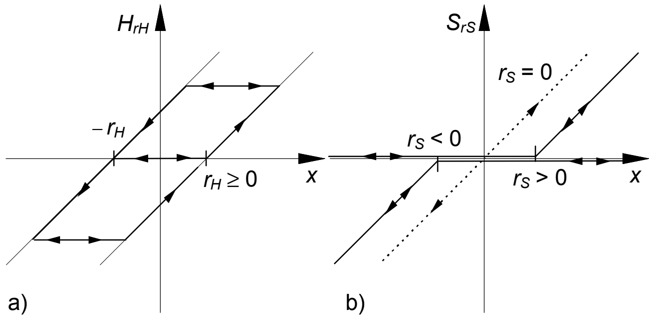


**Figure 2:** $x$-$y$-trajectory of the play (a) and the one-sided dead-zone operator (b)

The memory-less superposition operator $S$ describes the deviation of the real characteristic from the odd symmetry property of the operator $H$ [2,3]. It consists of the weighted linear superposition of $2l$+1 one-sided dead-zone operators $S_{rS}$, which are included in (16) in the $2l$+1-dimensional vector $\boldsymbol{S}_{rS}$. The rate-independent transfer characteristic is characterised by the threshold-dependent $x$-$y$-trajectory shown in fig. 2b. The weights $w_{Si}$ and the thresholds $r_{Si}$, $i = -l \,..\, +l$ of the one-sided dead-zone operators are considered in the vector notation (16) by the vector of weights $\boldsymbol{w}_S^{\,T} = (w_{S-l} \,..\, w_{S0} \,..\, w_{Sl})$ and the vector of thresholds $\boldsymbol{r}_S^{\,T} = (r_{S-l} \,..\, r_{S0} \,..\, r_{Sl})$ with $r_{S0} = 0$. The corresponding compensator

$$\begin{aligned}\Gamma^{-1}[y](t) &= H^{-1}[S^{-1}[y]](t)\\ &= \boldsymbol{w}_H'^{\,T} \cdot \boldsymbol{H}_{r_H'}[\boldsymbol{w}_S'^{\,T} \cdot \boldsymbol{S}_{r_S'}[y], \boldsymbol{z}_{H0}'](t)\end{aligned} \tag{17}$$

exists uniquely in the convex polyhedron

$$\Omega = \left\{ \begin{pmatrix} \boldsymbol{w}_H \\ \boldsymbol{w}_S \end{pmatrix} \in \begin{pmatrix} \Re^{n+1} \\ \Re^{2l+1} \end{pmatrix} \;\middle|\; \begin{pmatrix} \boldsymbol{U}_H & \boldsymbol{O} \\ \boldsymbol{O} & \boldsymbol{U}_S \end{pmatrix} \cdot \begin{pmatrix} \boldsymbol{w}_H \\ \boldsymbol{w}_S \end{pmatrix} - \begin{pmatrix} \boldsymbol{u}_H \\ \boldsymbol{u}_S \end{pmatrix} \ge \begin{pmatrix} \boldsymbol{o} \\ \boldsymbol{o} \end{pmatrix} \right\} \tag{18}$$

and follows from the inversion of $H$ and $S$ and the concatenation of $S^{-1}$ and $H^{-1}$ [2,3]. The matrices and vectors $\boldsymbol{U}_H \in \Re^{n+1\times n+1}$, $\boldsymbol{u}_H \in \Re^{n+1}$, $\boldsymbol{U}_S \in \Re^{2l+1\times 2l+1}$ and $\boldsymbol{u}_S \in \Re^{2l+1}$ in the inequality constraints in (18) are given by

$$\boldsymbol{U}_H = \begin{pmatrix} 1 & 0 & . & . & 0 \\ 1 & 1 & . & . & 0 \\ . & . & . & & . \\ . & . & & . & . \\ 1 & 1 & . & . & 1 \end{pmatrix}, \qquad \boldsymbol{u}_H = \begin{pmatrix} \varepsilon \\ \varepsilon \\ . \\ . \\ \varepsilon \end{pmatrix},$$

$$\boldsymbol{U}_S = \begin{pmatrix} 1 & \cdots & 1 & 1 & 0 & \cdots & 0 \\ \vdots & \ddots & \vdots & \vdots & \vdots & ⋰ & \vdots \\ 0 & \cdots & 1 & 1 & 0 & \cdots & 0 \\ 0 & \cdots & 0 & 1 & 0 & \cdots & 0 \\ 0 & \cdots & 0 & 1 & 1 & \cdots & 0 \\ \vdots & ⋰ & \vdots & \vdots & \vdots & \ddots & \vdots \\ 0 & \cdots & 0 & 1 & 1 & \cdots & 1 \end{pmatrix} \text{ and } \boldsymbol{u}_S = \begin{pmatrix} \varepsilon \\ \vdots \\ \varepsilon \\ \varepsilon \\ \varepsilon \\ \vdots \\ \varepsilon \end{pmatrix}.$$

$\varepsilon > 0$ is a lower bound and a design parameter which permits the change of strict inequality contraints by the inequality constraints in (18).

According to (17) the model structures of the Prandtl-Ishlinskii operators $H$ and $S$ are obviously invariable concerning the inversion operation. For the calculation of the inverse filter from the model and vice versa only the thresholds $\boldsymbol{r}_H$ and $\boldsymbol{r}_H$', the weights $\boldsymbol{w}_H$ and $\boldsymbol{w}_H$'and the initial values $\boldsymbol{z}_{H0}$ and $\boldsymbol{z}_{H0}$' have to be calculated by the corresponding mappings

$$\boldsymbol{w}_H' = \boldsymbol{\Phi}_H(\boldsymbol{w}_H) \qquad \text{or} \qquad \boldsymbol{w}_H = \boldsymbol{\Phi}_H(\boldsymbol{w}_H'), \tag{19}$$

$$\boldsymbol{r}_H' = \boldsymbol{\Psi}_H(\boldsymbol{r}_H, \boldsymbol{w}_H) \qquad \text{or} \qquad \boldsymbol{r}_H = \boldsymbol{\Psi}_H(\boldsymbol{r}_H', \boldsymbol{w}_H') \tag{20}$$

$$\boldsymbol{z}_{H0}' = \boldsymbol{\Theta}_H(\boldsymbol{z}_{H0}, \boldsymbol{w}_H) \qquad \text{or} \qquad \boldsymbol{z}_{H0} = \boldsymbol{\Theta}_H(\boldsymbol{z}_{H0}', \boldsymbol{w}_H') \tag{21}$$

$$\boldsymbol{w}_S' = \boldsymbol{\Phi}_S(\boldsymbol{w}_S) \qquad \text{or} \qquad \boldsymbol{w}_S = \boldsymbol{\Phi}_S(\boldsymbol{w}_S') \tag{22}$$

and

$$\boldsymbol{r}_S' = \boldsymbol{\Psi}_S(\boldsymbol{r}_S, \boldsymbol{w}_S) \qquad \text{or} \qquad \boldsymbol{r}_S = \boldsymbol{\Psi}_S(\boldsymbol{r}_S', \boldsymbol{w}_S'). \tag{23}$$

The derivation of these mappings is not the aim of this article. For this purpose we refer to the original papers [2,3].

### 3.1 Generalised error model

The invariability of the Prandtl-Ishlinskii operators $H$ and $S$ refering to the inversion operation makes it possible to generate a generalised error model

$$\begin{aligned} E[x,y](t) &= H[x](t) - S^{-1}[y](t) \\ &= \boldsymbol{w}_H{}^T \cdot \boldsymbol{H}_{r_H}[x, \boldsymbol{z}_{H0}](t) - \boldsymbol{w}_S'^T \cdot \boldsymbol{S}_{r_S'}[y](t) \end{aligned} \tag{24}$$

which depends linearly on the weights $\boldsymbol{w}_H$ and $\boldsymbol{w}_S$'. This generalised error model is the starting point for the synthesis of the modified Prandtl-Ishlinskii hysteresis operator $\Gamma$ and its compensator $\Gamma^{-1}$ starting from the measured input signal $x(t)$ and output signal $y(t)$. For the real values $\boldsymbol{r}_H$, $\boldsymbol{w}_H$, $\boldsymbol{z}_{H0}$, $\boldsymbol{r}_S'$, $\boldsymbol{w}_S'$ of the generalised error model follows

$$E[x,y](t) = w_{H0}\left(\frac{\boldsymbol{w}_H{}^T}{w_{H0}} \cdot \boldsymbol{H}_{r_H}[x, \boldsymbol{z}_{H0}](t) - \frac{\boldsymbol{w}_S'^T}{w_{H0}} \cdot \boldsymbol{S}_{r_S'}[y](t)\right) = 0$$

for all $t$ and $w_{H0} > 0$. Therefore the expression between the parentheses has to be zero for all times. Thus the error model is overdetermined with one degree of freedom and consequently $w_{H0} = 1$ can be given as a real value. With $x = H_{rH0}[x, z_{H00}]$ follows the alternative representation

$$\begin{aligned} E[x,y](t) &= x(t) + \begin{pmatrix} \boldsymbol{w}_G{}^T & \boldsymbol{w}_S'^T \end{pmatrix} \cdot \begin{pmatrix} \boldsymbol{G}_{r_G}[x, \boldsymbol{z}_{G0}](t) \\ -\boldsymbol{S}_{r_S'}[y](t) \end{pmatrix} \\ &= x(t) + \boldsymbol{w}^T \cdot \boldsymbol{\Psi}[x,y](t). \end{aligned} \tag{25}$$

The $n$-dimensional vectors $\boldsymbol{r}_G$, $\boldsymbol{w}_G$, $\boldsymbol{z}_{G0}$ und $\boldsymbol{G}_{rG}$ result from the $n$+1-dimensional vectors $\boldsymbol{r}_H$, $\boldsymbol{w}_H$, $\boldsymbol{z}_{H0}$ and $\boldsymbol{H}_{rH}$ by cancelling the first components. The weights $\boldsymbol{w}_G \in \Re^n$ and $\boldsymbol{w}_S' \in \Re^{2l+1}$ in (25) are combined in the vector $\boldsymbol{w} \in \Re^d$ and the output signals $\boldsymbol{G}_{rG}[x, \boldsymbol{z}_{G0}](t) \in \Re^n$ and $-\boldsymbol{S}_{r'S}[y](t) \in \Re^{2l+1}$ of the elementary operators are combined in the signal vector $\boldsymbol{\Psi}[x,y](t) \in \Re^d$ with $d = n+2l+1$. Starting from the generalised error model synthesis of the modified Prandtl-Ishlinskii hysteresis operator $\Gamma$ and its compensator $\Gamma^{-1}$ is realised in four steps.

### 3.2 Determination of the error model parameters

In the first synthesis step the thresholds $\boldsymbol{r}_G$ and $\boldsymbol{r}_S$' and the initial values $\boldsymbol{z}_{G0}$ are determined by the formulas

$$r_{Gi} = \frac{i}{n+1} \max_{0 \le t \le t_E} \{|x(t)|\} \quad ; \quad i = 1 \,..\, n, \tag{26}$$

$$\begin{aligned} r_{Si}' &= \frac{i}{l+1} \min_{0 \le t \le t_E} \{y(t)\} \quad ; \quad i = -l \,..\, -1 \\ r_{Si}' &= \frac{i}{l+1} \max_{0 \le t \le t_E} \{y(t)\} \quad ; \quad i = +0 \,..\, +l \end{aligned} \tag{27}$$

and

$$z_{G0i} = 0 \quad ; \quad i = 1 \,..\, n. \tag{28}$$

In addition to the the model orders $n$ and $l$, the maximum of the absolute value of the measured input signal and the maximum and minimum value of the output signal must be given. Moreover, during identification (28) assumes the evolution of the hysteretic state from the so-called „virgin“ or „demagnetised“ state.

The determination of the weights is the aim of the second step and follows from the least-square minimisation of the generalised error model (25), which means by the solution of the bounded quadratic optimisation problem (1) - (3) with

$$\begin{aligned} \boldsymbol{H} &= \int_0^{t_E} \boldsymbol{\Psi}[x,y](t) \boldsymbol{\Psi}[x,y](t)^T \mathrm{d}t, \\ \boldsymbol{g} &= +\int_0^{t_E} x(t) \boldsymbol{\Psi}[x,y](t) \ \mathrm{d}t, \\ f &= +\frac{1}{2} \int_0^{t_E} x^2(t) \ \mathrm{d}t \end{aligned} \tag{29}$$

and

$$\boldsymbol{U} = \begin{pmatrix} \boldsymbol{U}_G & \boldsymbol{O} \\ \boldsymbol{O} & \boldsymbol{U}_S \end{pmatrix}, \ \boldsymbol{u} = \begin{pmatrix} \boldsymbol{u}_G \\ \boldsymbol{u}_S \end{pmatrix}. \tag{30}$$

The matrix $\boldsymbol{U}_G \in \Re^{n \times n}$ in (30) results from $\boldsymbol{U}_H$ by cancelling the first row and column. The vector $\boldsymbol{u}_G \in \Re^n$ in (30) results from cancelling the first component of $\boldsymbol{u}_H - \boldsymbol{i}$ with $\boldsymbol{i}^T = (1 \ 1 \ .. \ 1) \in \Re^{n+1}$. (3) and (30) guarantee the existence of the operators $H^{-1}$ and $S$ starting from the operators $H$ and $S^{-1}$ and vice versa and thus the applicability of the transformation mappings (19-23). According to section 2 the quadratic program (1) - (3) with (29) and (30) can be solved by the numerical time-integration of the differential equation (10). For this purpose the initial values of (10) must lie within the feasible region. A meaningful assumption for the determination of the initial values is to have no information about the hysteretic nonlinearity. In this case it is meaningful to choose the initial values for the error model in such a way that the model $\Gamma$ and its compensator $\Gamma^{-1}$ exhibit the behaviour of the identity operator $I$. From this idea follows the initial values $\boldsymbol{w}_{G0}{}^T = (0\ 0\ .\ .\ 0) \in \Re^n$ and $\boldsymbol{w}_{S0}' = (0\ .\ .\ 0\ 1 = w_{S00}\ 0\ .\ .\ 0) \in \Re^{2l+1}$.

According to section 2 the stability properties of the differential equation depend decisively on the definiteness properties of the Hessian matrix $\nabla\nabla V$. If the inequality

$$\int_0^{t_E} \left(\boldsymbol{\Psi}[x,y](t)^T \cdot \boldsymbol{w}\right)^2 \mathrm{d}t > 0 \quad \forall\ \boldsymbol{w} \in \Re^d \setminus \{\boldsymbol{o}\} \tag{31}$$

is fulfilled the Hessian matrix $\nabla\nabla V$ is positive-definite and there exists exactly one globally exponentially stable equilibrium point $\boldsymbol{w}_\infty$, which is also the unique global mimimum value $\boldsymbol{w}_*$ of the optimisation problem (1) - (3). Condition (31) demands the nonexistence of any vector of weights apart from the zero vector which is perpendicular to the signal vector generated by the elementary operators for all $0 \le t \le t_E$. This condition is fulfilled if the components of the signal vector are all different from zero and moreover linearly independent in the interval $0 \le t \le t_E$. The latter condition is given by the fact that because of (26-27) the elementary operators in the signal vector have different thresholds. The former condition requires the crossing of every threshold $r_{Gi}$, $i = 1\ .\ .\ n$ and $r_S{}'_i$, $i = -l\ .\ .\ l$ by the amplitudes of the input signal $x(t)$ and the output signal $y(t)$. Because of (26-27) this property of the input and output signal is given a-priori as well.

### 3.3 Model and compensator synthesis

In the third step the parameters of the identified Prandtl-Ishlinskii hysteresis operator $H$ have to be completed by

$$\boldsymbol{w}_H{}^T = (1 \quad \boldsymbol{w}_G{}^T), \tag{32}$$

$$\boldsymbol{r}_H{}^T = (0 \quad \boldsymbol{r}_G{}^T), \tag{33}$$

and

$$\boldsymbol{z}_{H0}{}^T = (x_0 \quad \boldsymbol{z}_{G0}{}^T). \tag{34}$$

In the fourth step the corresponding model $\Gamma$ and the corresponding compensator $\Gamma^{-1}$ are generated by the transformation mappings (22-23) and (19)-(21), respectively.

## 4 Results

The procedure for the design of inverse hysteretic filters with projected dynamical systems was tested by means of the measured complex hysteretic displacement-voltage relationship $W$ of a piezoelectric stack transducer shown in fig. 3 as a black curve. The voltage $U$ of the transducer is the system input $x$ and the displacement $s$ the system output $y$. For the modeling of the measured characteristic a modified Prandtl-Ishlinskii hysteresis operator $\Gamma$ with a model order of $n = 7$ and $l = 3$ was used. This model order results in a number of $n+1 = 8$ play operators for modeling the hysteretic memory and $2l+1 = 7$ one-sided deadzone operators for modeling the memory-free saturation characteristic. The maximum of the absolute value of the measured input voltage amounts in this case to 500 V. The minimum and the maximum of the measured displacement signal are −24.08 µm and +19.38 µm. The threshold values $\boldsymbol{r}_H$ and $\boldsymbol{r}_S'$ of the generalised error model $E$ are shown in table 1.

| $i$ | $r_H$ | $w_H$ | $r_H'$ | $w_H'$ |
|---|---|---|---|---|
| 0 | $+0.00\cdot10^{+0}$ | $+1.00\cdot10^{+0}$ | $+0.00\cdot10^{+0}$ | $+1.00\cdot10^{+0}$ |
| 1 | $+6.25\cdot10^{+1}$ | $+2.76\cdot10^{-1}$ | $+6.25\cdot10^{+1}$ | $-2.16\cdot10^{-1}$ |
| 2 | $+1.25\cdot10^{+2}$ | $+1.57\cdot10^{-1}$ | $+1.42\cdot10^{+2}$ | $-8.60\cdot10^{-2}$ |
| 3 | $+1.88\cdot10^{+2}$ | $+1.60\cdot10^{-1}$ | $+2.32\cdot10^{+2}$ | $-7.00\cdot10^{-2}$ |
| 4 | $+2.50\cdot10^{+2}$ | $+1.18\cdot10^{-1}$ | $+3.31\cdot10^{+2}$ | $-4.33\cdot10^{-2}$ |
| 5 | $+3.13\cdot10^{+2}$ | $+1.22\cdot10^{-1}$ | $+4.38\cdot10^{+2}$ | $-3.88\cdot10^{-2}$ |
| 6 | $+3.75\cdot10^{+2}$ | $+6.12\cdot10^{-2}$ | $+5.53\cdot10^{+2}$ | $-1.77\cdot10^{-2}$ |
| 7 | $+4.38\cdot10^{+2}$ | $+1.78\cdot10^{-1}$ | $+6.71\cdot10^{+2}$ | $-4.54\cdot10^{-2}$ |

| $j$ | $r_S$ | $w_S$ | $r_S'$ | $w_S'$ |
|---|---|---|---|---|
| −3 | $-6.14\cdot10^{+2}$ | $+1.50\cdot10^{-3}$ | $-1.81\cdot10^{+1}$ | $-1.46\cdot10^{+0}$ |
| −2 | $-4.21\cdot10^{+2}$ | $+2.07\cdot10^{-3}$ | $-1.20\cdot10^{+1}$ | $-2.27\cdot10^{+0}$ |
| −1 | $-2.15\cdot10^{+2}$ | $+1.17\cdot10^{-3}$ | $-6.02\cdot10^{+0}$ | $-1.44\cdot10^{+0}$ |
| 0 | $+0.00\cdot10^{+0}$ | $+2.69\cdot10^{-2}$ | $+0.00\cdot10^{+0}$ | $+3.72\cdot10^{+1}$ |
| +1 | $+1.87\cdot10^{+2}$ | $-6.52\cdot10^{-4}$ | $+4.85\cdot10^{+0}$ | $+1.00\cdot10^{+0}$ |
| +2 | $+3.80\cdot10^{+2}$ | $-1.37\cdot10^{-3}$ | $+9.69\cdot10^{+0}$ | $+2.29\cdot10^{+0}$ |
| +3 | $+5.83\cdot10^{+2}$ | $-1.24\cdot10^{-3}$ | $+1.45\cdot10^{+1}$ | $+2.31\cdot10^{+0}$ |

**Table 1:** Weights and threshold values of the modified Prandtl-Ishlinskii hysteresis operator $\Gamma$ and its corresponding inverse $\Gamma^{-1}$

After the synthesis of the matrix $\boldsymbol{H}$, the vector $\boldsymbol{g}$ and the scalar $f$ by means of the measured data according to (25) and (29) the weights $\boldsymbol{w}_H$ and $\boldsymbol{w}_S'$ of the generalised error model $E$ are determined through the time-integration of the corresponding projected dynamical system (10). Due to the bounded space the discussion of the time-discrete scheme for the numerical solution of (10) is beyond the scope of this article. A detailed discussion of this topic can be found in [4]. The equilibrium point $\boldsymbol{w}_\infty$ of the weight vector $\boldsymbol{w}^T = (\boldsymbol{w}_G{}^T, \boldsymbol{w}_S'^T)$ is given by the vector $\boldsymbol{w}_S'$ and the components $w_{Hi}$, $i = 1\ .\ .\ n$ of the vector $\boldsymbol{w}_H$ shown in table 1. The vectors $\boldsymbol{r}_H$ and $\boldsymbol{w}_H$ in table 1 represent the completion of the vectors $\boldsymbol{r}_G$ and $\boldsymbol{w}_G$ according to (32) - (33). The thresholds $\boldsymbol{r}_S$ and the weights $\boldsymbol{w}_S$ in table 1 result from the transformation mappings (22) - (23) and are together with the thresholds $\boldsymbol{r}_H$ and the weights $\boldsymbol{w}_H$ the parameter base for the modified Prandtl-Ishlinskii hysteresis operator $\Gamma$. As shown in fig. 3 as a dark grey curve the trajectory of $\Gamma$ is in good agreement with the measured characteristic $W$. The thresholds $\boldsymbol{r}_H'$ and the weights $\boldsymbol{w}_H'$ in table 1 result from the transformation mappings (19) - (20). They determine together with the thresholds $\boldsymbol{r}_S'$ and the weights $\boldsymbol{w}_S'$ the transfer characteristic of the compensator $\Gamma^{-1}$. The trajectory of $\Gamma^{-1}$ is shown in fig. 3 as a grey curve. The light grey curve in fig. 3 displays the compensation effect of a feedforward control scheme $s = \Gamma^{-1}[W[s_c]]$ with $s_c$ as the given displacement signal. This results in a strong linearisation of the hysteretic actuator charateristic of the piezoelectric transducer.

As an example fig. 4 shows the evolution of the error-model parameter $w_{G0}$ in time for the optimisation with the corresponding projected dynamical system (10) as a solid line and with the differential equation (7) which is the couterpart of (10) for the unconstrained case as a dashed line.

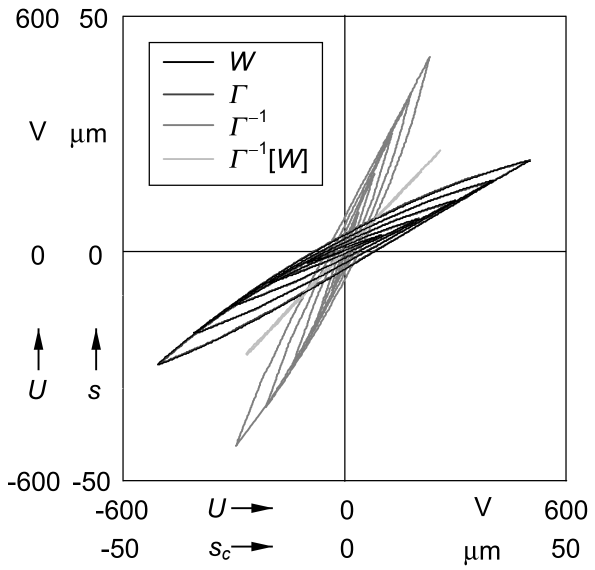


**Figure 3:** Modified Prandtl-Ishlinskii operator $\Gamma$ and the corresponding inverse $\Gamma^{-1}$ for a typical measured piezoelectric actuator characteristics $W$

The grey shaded area in fig. 4 marks a parameter region where the inequality contraints in (3) are violated and thus the existence of a compensator $\Gamma^{-1}$ fails. The time-integration of (7) leads to a time evolution of $w_{G0}$ which produces a time intervall for which the compensator $\Gamma^{-1}$ does not exist. This is a crucial property for every iterative learning compensation strategy which uses the above identification scheme for the on-line compensator synthesis.

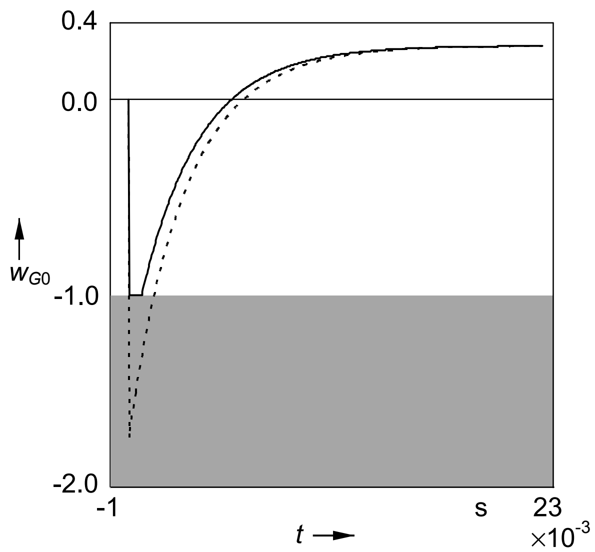


**Figure 4:** Evolution of the error-model parameter $w_{G0}$ in time

In contrast to (7) the time integration of (10) produces a time evolution of $w_{G0}$ which slides along the boundary of the feasibility set $K$ where the time-integration of (7) crosses the boundary. As a consequence of the projection mechanism in (10) the compensator $\Gamma^{-1}$ exists at all times. This is an essential assumption for the design of an iterative learning compensation strategy for complex hysteretic nonlinearities based on the synthesis procedure described in section 3.

## 5 Summary and prospects

The present paper describes a procedure for synthesising an inverse filter for a complex hysteretic nonlinearity as it occurs in active materials such as piezoelectric ceramics, magnetostrictive materials and shape memory alloys using the so-called modified Prandtl-Ishlinskii approach. In this synthesis procedure the parameters of an appropriate linear error model have to be optimised in a convex polyhedron to ensure the existence of the corresponding inverse filter. As in future work concerned with iterative and adaptive compensation strategies the determination of the parameters should be performed on-line, the solution of the underlying convex quadratic programming problem is formulated as the global exponentially stable equilibrium point of a properly projected dynamical system. In contrast to the formulation of the on-line optimisation process as an unconstrained dynamical system the formulation as a projected dynamical system ensures the existence of the inverse filter at all times.


## Acknowledgement

The author thanks Prof. Dr.-Ing. habil. Hartmut Janocha from the Laboratory for Process Automation (LPA) at Saarland University in Saarbrücken and Dr. Pavel Krejci from the Mathematical Institute of the Academy of Sciences in Prague for the support of this project.


## References


[1] K. Kuhnen, H. Janocha. „Complex hysteresis modeling of a broad class of hysteretic actuator nonlinearities“, *8th Int. Conf. on New Actuators*, Bremen, pp. 688-691, (2002).

[2] K. Kuhnen. „Inverse Steuerung piezoelektrischer Aktoren mit Hysterese-, Kriech- und Superpositionsoperatoren“, *Doctoral Thesis*, *Saarland University*, *Shaker Verlag*, Aachen, (2001).

[3] K. Kuhnen. „Modelling, Identification and Compensation of Complex Hysteretic Nonlinearities - A modified Prandtl-Ishlinskii approach“, *European Journal of Control*, accepted for publication.

[4] A. Nagurney, D. Zhang. „Projected dynamical systems and variational inequalities with applications“, *Kluwer Academic Publishers*, Dortrecht, (1996).

[5] M. Papageorgiou. „Optimierung“, *Oldenbourg Verlag*, München, (1991).

[6] G. Webb, A. Kurdila, D. Lagoudas. „Adaptive Hysteresis Model for Model Reference Control with Actuator Hysteresis“, *Journal of Guidance, Control and Dynamics*, **Vol. 23**, **No. 3**, pp. 459-465, (2000).